ELSEVIER

Journal of Nuclear Materials 288 (2001) 137–147

journal of nuclear materials

www.elsevier.nl/locate/jnucmat

On the role of grain boundary diffusion in fission gas release

D.R. Olander [a,*], P. Van Uffelen [b]

[a] *Department of Nuclear Engineering, University of California, Berkeley, CA 94720-1730, USA*
[b] *Department of Reactor Materials Research, SCK·CEN, Boeretang 200, B-2400 Mol, Belgium*

Received 26 January 2000; accepted 2 November 2000

Abstract

It is generally believed that thermal fission gas release from LWR fuel occurs mainly via interconnected grain boundary bubbles. Grain boundary diffusion is not considered to be a significant mechanism. We investigated this supposition by two methods; first, by assessing the distance a gas atom can migrate in a grain boundary containing perfectly absorbing traps. For areal number densities and fractional coverages by the traps observed in fuel irradiated to burnups exceeding ~ 20 MWd/kg, gas atoms will be trapped after a migration distance equal to the size of a grain or less. This supports the supposition for medium-to-high burnups. However, the above-mentioned model is inapplicable for trace-irradiated specimens. In our second analysis, we examined Xe release from trace-irradiated UO_2. The measurements indicated that the liberation involves more than only lattice diffusion at the specimen surface, and that the data are consistent with sequential lattice and grain boundary diffusion unimpeded by intergranular traps. The analysis also provided rough estimates of the grain boundary diffusion coefficient in UO_2.

PACS: 28.41.Ak; 61.72.Mm; 61.72.Qq; 66.30.Jt

1. Introduction

Impurity migration by diffusion along grain boundaries is a well-known phenomenon in polycrystalline metals [1,2]. In nuclear fuels, the same process is believed to assist transport of oxygen [3], burnable poisons [4], and plutonium [5]. Turnbull et al. [6–8] presented experimental evidence and a theoretical model demonstrating enhancement of the release of the volatile fission products Te and I by grain boundary diffusion in low burnup fuel.

Transport of the fission gases Xe and Kr present a much more confused picture. Early evidence [9] from in-pile release experiments at 0.1% burnup showed that Xe was significantly more mobile in single-crystal UO_2 than in standard polycrystalline material. This observation was attributed to natural traps for fission gas atoms in the grain boundary; intergranular bubble formation was not reported. On the basis of similar in-pile tests, Turnbull and Friskney [6] excluded Xe from the group of volatile fission products whose release is aided by grain boundary diffusion. They observed no difference in the release-to-birth rate ratio between single-crystal and polycrystalline UO_2 specimens. Rather than acting as traps, Turnbull et al. considered this observation to mean that the grain boundaries in UO_2 offered the same mobility to fission gases as the lattice of the grains.

Although we know of no experimental evidence that demonstrates enhanced release due to diffusion of Xe in the grain boundaries of UO_2, numerous sources (including one of the present authors) have claimed that grain boundaries in nuclear fuel are 'fast transport paths' even in the absence of interlinked porosity. This belief is in part at least due to the pervasive and persistent influence of Booth's model [10], in which fission gas release is completely controlled by intragranular diffusion in an 'equivalent sphere'. The physical entity often associated with Booth's equivalent sphere is the grain. This assignment of the rate-controlling step to

* Corresponding author. Tel.: +1-510 642 7055; fax: +1-510 643 9685.
E-mail address: fuelpr@cmsa.berkeley.edu (D.R. Olander).

0022-3115/01/$ - see front matter
PII: S0022-3115(00)00725-X

intragranular diffusion then requires that the grain boundaries offer no resistance to Xe transport to free surfaces. This picture is often justified by the common observation that fission gas release decreases as the grain size increases. While this effect is clearly consistent with the Booth model, it is no proof of the model. For example, the same behavior would occur if intragranular diffusion were rapid and the release process were controlled entirely by diffusion in the grain boundaries (because a larger grain size reduces the number of grain boundaries available for solute transport).

An example of the implicit assumption of rapid grain boundary transport can be found in [11], in which release from the grains is equated to release from the fuel. Another example is the VICTORIA code [12], which treats release from the grains as tantamount to release to natural internal porosity (not the kind produced by interlinked gas bubbles on grain boundaries). Olander modeled transport in polycrystalline UO_2 of solute species with known lattice/grain boundary segregation coefficients [13] and subsequently included grain growth and a distribution of grain sizes [14]. The models were applied to freely migrating solute atoms confined to grain boundaries. The error in these papers was considering fission gas to represent this class of solute. Guérin et al. [15] claim to have experimental evidence of long-range grain boundary diffusion of fission gas in the U-rich oxide component of MOX fuel. This assertion is based on the lower-than-expected gas content of the central portions of PWR rods, despite the absence of interconnected bubbles, or bubbles of any kind. Although plausible, this explanation is only a hypothesis, not a mechanistic demonstration. The justification given by Guérin et al. is based on the known higher cation grain boundary diffusion coefficient in mixed oxide compared to UO_2. However, this fact cannot be transferred to electrically neutral gas species for the same reason that Te, I, and Cs intergranular mobility is not reflected by Xe.

Fission gas release measurements on irradiated PWR fuel rods from numerous sources all show essentially no gas release until a threshold burnup of ~ 20 MWd/kg U, with variations depending on power history. The general consensus explaining this observation is that during the incubation period, all gas arriving at the grain boundaries is trapped locally. The intergranular gas concentration increases with burnup until grain-face bubbles are nucleated. Growth of these bubbles eventually results in interlinkage, thereby triggering the gas release process. This picture is faithfully reflected in all known fission-gas release codes (e.g. [16–22]), none of which includes grain-boundary diffusion as a release mechanism, as well as microscopic observations of irradiated fuels [23–27].

Although long-range intergranular Xe diffusion in UO_2 is effectively inhibited, the short-range analog may occur in order to nucleate and grow grain-face bubbles from the atoms arriving from the grain. Such a local atomic transport mechanism has been invoked by Kogai [28]. In view of the absence of any measurement of D_{gb} of Xe in UO_2, Kogai had to resort to using the value for U^{4+}.

Given the state of affairs described above, the purpose of the present work is to provide a partial answer to the question: 'Why is Xe unique in its immobility in the grain boundaries of UO_2?' The short answer is that Xe is neutral, whereas the other species are ionic [29]. Agglomeration of Xe into bubbles in UO_2 is not only possible, it is energetically favored. On the other hand, precipitation of ionic species is restricted (and probably hindered) by electrical neutrality requirements. However, the molecular dynamic calculations needed to quantitatively demonstrate this hypothesis for grain boundaries remain to be performed.

The present work seeks to answer two more modest questions germane to the above general topic, namely:

1. How far can a Xe atom migrate in a grain boundary containing a specific population of traps before being captured in one of the traps?
2. If the answer to the first question is 'not far', how does Xe escape from polycrystalline UO_2 in the period preceding interlinkage of intergranular gas bubbles?

2. Migration distance by diffusion theory

In order to answer the first question using conventional diffusion theory, the characteristics of the trap population on the grain boundaries need to be specified. Circular traps of radius R and number density N (per unit area) are assumed to be arranged on a square pattern on the boundary. The circular unit cell with a single trap at its center has a radius R_o given by

$$R_o = (\pi N)^{-1/2}. \tag{1}$$

The traps occupy a fraction ϕ of the grain face given by

$$\phi = \pi R^2 N = (R/R_o)^2. \tag{2}$$

The detailed nature of the traps need not be specified; in lightly-irradiated UO_2, they may consist of segregated impurity clusters, precipitates, dislocation walls, or structural nonuniformities on the crystal face of the grain. In more heavily irradiated fuel, the dominant traps are precipitated fission gas bubbles or solid fission product precipitates.

Apart from the geometric features given above, the only relevant physical property of the trap is its capture efficiency for particular types of solutes migrating as single atoms in the boundary. A highly efficient trap absorbs all solute reaching its periphery, and so reduces

the concentration of the solute to zero at this location. If the trap is less efficient in capturing arriving solute atoms, the concentration of the latter at the trap surface is greater than zero. In general, the greater the capture efficiency of the trap, the shorter the distance that a solute atom can move before being removed by trapping and the greater is the impediment to release. Since this paper is directed towards fission gas behavior, the capture efficiency is assumed to be high. Extension of the model to low-efficiency trapping, which would better reflect the behavior of the other volatile fission products, is given in [30].

To determine the migration distance of fission gas atoms in a field of traps on the grain boundary, we first assess their lifetime by solving the transient diffusion problem in the annular unit cell $R \leqslant r \leqslant R_o$. The diffusion equation in cylindrical coordinates contains a source term S representing arrival of solute from the grains but neglects radiation re-solution. The initial condition is zero concentration in the unit cell, and the boundary conditions are zero concentration at $r = R$ and zero gradient at $r = R_o$. The solution can be written in the form [31]

$$c(r,t) = c_{ss}(r) - \frac{S}{\pi D_{gb}} \sum_{n=0}^{\infty} \Omega_n(r) e^{-t/\tau_n}, \tag{3}$$

where $c_{ss}(r)$ is the steady-state concentration distribution and D_{gb} is the gas-atom diffusion coefficient in the boundary. The eigenfunctions are denoted by $\Omega_n(r)$ and the eigenvalues are expressed in terms of characteristic times τ_n. The latter are determined by the transcendental equation involving Bessel functions of the first and second kind:

$$J_0\left(\frac{R}{\sqrt{D_{gb}\tau_n}}\right) Y_1\left(\frac{R_o}{\sqrt{D_{gb}\tau_n}}\right) = Y_0\left(\frac{R}{\sqrt{D_{gb}\tau_n}}\right) J_1\left(\frac{R_o}{\sqrt{D_{gb}\tau_n}}\right), \quad \text{where } n = 0, 1, 2 \ldots \tag{4}$$

The longest characteristic time τ_0 is interpreted as the mean lifetime of a fission gas atom in the grain boundary [32]. That is, it represents the average time interval between arrival of a gas atom from the grain and its capture by a grain boundary trap.

The lifetime is converted to a mean migration distance using the solution of the diffusion problem for a point source in an infinite plane:

$$L = 2\sqrt{D_{gb}\tau_0}. \tag{5}$$

Substituting Eqs. (2) and (5) into Eq. (4) yields

$$J_0\left(2\frac{R_o}{L}\sqrt{\phi}\right) Y_1\left(2\frac{R_o}{L}\right) = Y_0\left(2\frac{R_o}{L}\sqrt{\phi}\right) J_1\left(2\frac{R_o}{L}\right), \tag{6}$$

from which the ratio L/R_o can be computed as a function of ϕ. Note that the migration length is independent of the grain boundary diffusion coefficient and depends only upon the two geometric properties of the trap population, R_o and ϕ, or, equivalently, N and ϕ.

3. Migration distance by random-walk theory

In order to extend the analysis of Section 2 to a random array of traps, the same problem is treated in this section by random-walk methods. The circular traps are placed randomly on a planar grid representing the field on which Xe atoms jump randomly from site to site. The distance between sites on the grid is the diffusive jump distance, α, which is approximately equal to the lattice constant.

A fission gas atom arriving from the grain either hits a trap and is absorbed or lands on a site from which the random walk begins. Subsequently, capture by a trap occurs if the jumps land the atom on one of the peripheral sites of the trap, of which there are approximately $(2\pi R/\alpha)N$ per unit grain boundary area. Since the interior of the traps is forbidden, the number of sites (per unit area) available for jumping is $\alpha^{-2} - (\pi R^2/\alpha^2)N$. If all jumps are randomly directed, the probability of capture per jump, p, is the ratio of the above site densities. Using Eq. (2) to eliminate N yields

$$p = \frac{2\phi}{1-\phi}\left(\frac{\alpha}{R}\right). \tag{7}$$

Because both ϕ and α/R are small, $p \ll 1$. The probability that a Xe atom survives j jumps on the grain boundary is $(1-\phi)(1-p)^j$. The first term in this product is the probability that the Xe atom misses a trap upon arriving from the grain. The average number of jumps before capture is the j-weighted sum:

$$\bar{j} = \sum_{j=1}^{\infty} j(1-\phi)(1-p)^j = (1-\phi)(1-p)/p^2 \approx (1-\phi)/p^2.$$

From random-walk theory, the crow-flight distance traveled by an atom in this number of jumps is $L = \sqrt{\bar{j}\alpha^2}$. Eliminating p in the above equation using Eq. (7) and expressing R in terms of ϕ and N by Eq. (2) yields

$$L = \frac{1}{2\sqrt{\pi N}} \frac{(1-\phi)^{3/2}}{\sqrt{\phi}}. \tag{8}$$

As in the diffusion theory analysis in Section 2, Eq. (8) can be modified for inefficient trapping. This is accomplished by assigning a probability <1 that a Xe atom reaching a trap's peripheral site is absorbed, as described in [30].

4. The mechanism of fission gas release prior to bubble interlinkage

The migration lengths given by Eqs. (6) and (8) are shown in Figs. 1 and 2, respectively. The range of N and ϕ in Figs. 1 and 2 represent those observed for gas bubbles in fractography of irradiated fuel [33,34]. The two calculation methods are in good agreement at large trap fractional coverages but deviate by more than a factor of two at the combination of low trap density and small fractional coverage. Despite this difference, both methods show that in this parameter space the migration distance of Xe is too small for grain boundary diffusion to free surfaces to contribute to gas release. There remains, however, the fundamental question of whether grain boundary diffusion contributes to fission gas release at burnups below the threshold for intergranular bubble nucleation. More precisely, are there natural traps in fresh UO_2 that perform the same function as bubbles in irradiated fuel?

There have been no microstructural observations of defects that could serve as natural traps for fission gases on grain boundaries in unirradiated UO_2. Nonetheless, natural traps may be responsible for impeding (but not preventing) gas release from trace-irradiated lab specimens or low-burnup power reactor fuel. If the N–ϕ combinations that characterize the natural traps are significantly smaller than those in Figs. 1 and 2, the Xe migration distance along grain boundaries could be large enough to permit long-range fission gas diffusion on grain boundaries to contribute significantly to the release process.

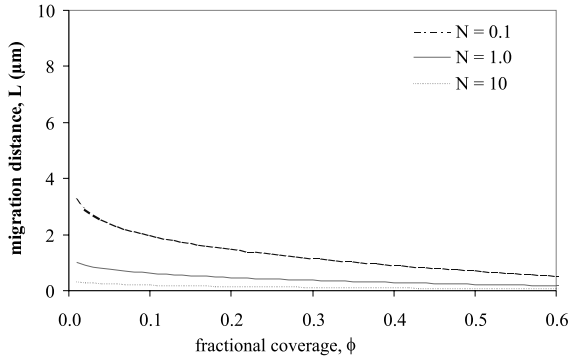

Fig. 1. Fission gas migration distance from diffusion theory.

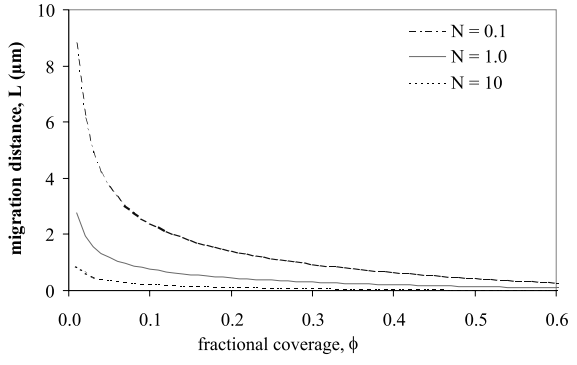

Fig. 2. Fission gas migration distance from random-walk model.

Gas release from trace-irradiated specimens and from low-burnup fuel is small but not zero. In typical PWR fuel, fractional Xe releases are $\sim 0.1\%$ at 10 MWd/kg U and rise rapidly at burnups in excess of ~ 20 MWd/kg U [15]. The accelerated release at high burnup (which also occurs during transients) is believed to be due to intergranular bubble formation and interlinkage. The low-burnup release results from recoil and knockout with a diffusional contribution from the hottest parts of the fuel.

Analysis of post-irradiation annealing experiments on trace-irradiated UO_2 specimens provides an excellent method of determining whether grain boundary diffusion is active in xenon release. Trace-irradiated specimens have no intergranular bubbles and are at a uniform temperature during gas release. A consistent observation in these experiments is the higher apparent diffusivity of Te and I compared to Xe, often by as much as a factor of 100 [6,35,36]. These species-dependent differences have been interpreted as a consequence of more effective trapping of Xe in grain boundaries than of the other volatile fission products. These latter species are thereby free to utilize the grain boundaries as fast-diffusion pathways to free surfaces.

To test this notion, previously published data on fission-gas release from trace-irradiated, stoichiometric UO_2 by Mansouri and Olander [36] are re-examined to ascertain whether they contain any evidence of grain-boundary-assisted release of fission gas. In these experiments, the specimens were disks cut from reactor fuel pellets to thicknesses of 0.9–1.5 mm and irradiated to a fractional burnup of 10^{-8}. This dose is well below the value at which radiation effects on the diffusion coefficient appear. Prior to irradiation and during the subsequent post-irradiation annealing, the specimens were maintained in a H_2/Ar atmosphere that maintained the stoichiometry at exactly 2.00. Five data points were obtained at anneal temperatures ranging from 1400°C to 1700°C. Release fractions were obtained by measuring the 81-keV photopeak of Xe for the released gas collected in liquid-nitrogen-cooled charcoal and comparing the intensity to that of the same peak in the original disk specimen.

The question is how to analyze these five data points. One approach is to utilize the theory of combined grain-boundary and lattice diffusion developed in [13] and modified to include trapping of Xe in the grain boundaries. The transport parameters to be fitted to the data in

such an approach are the pre-exponential factors and activation energies of the lattice and grain-boundary diffusion coefficients. In addition, N and ϕ introduced in Section 2 to characterize the intergranular traps need to be fitted in the model. However, fitting five data points to a model with six parameters cannot produce believable results; the number of unknowns to be fitted to the data needs to be reduced. This can be accomplished by fixing the lattice diffusion coefficient from literature data and fitting the release data with only the two grain-boundary diffusivity parameters and a third parameter obtained by collapsing the two intergranular trap morphology parameters into a single quantity.

Unfortunately, the lattice diffusivity of Xe in UO_2 is not well established; Matzke's review [37], for example, presents several data sets covering a spread of a factor of 100 in D at 1400°C (from 10^{-14} to 10^{-12} cm^2/s). In addition, many fission gas release/swelling models utilize older lattice diffusivity data obtained by Davies and Long [38], which is even lower (5×10^{-15} cm^2/s at 1400°C) than those in Matzke's review. By far the lowest value of D was reported by Cornell [39]; at 1400°C, his value is 3×10^{-16} cm^2/s. In order to narrow this vast range, the two extreme results are rejected and two intermediate cases are used. The first, representing 'low' values, is the Davies and Long [38] equation:

$$D = 7.6 \times 10^{-6} \exp(-293/RT), \tag{9}$$

where D is in cm^2/s, the activation energy in kJ/mol, and $R = 8.315$ J/K mol. The 'high' value is taken to be the composite based on three sets of data reported in Matzke's paper (called the 'Xe low concentration' line in Fig. 8 of [37]):

$$D = 1.0 \times 10^{-4} \exp(-289/RT). \tag{10}$$

The two equations give D values differing by slightly more than an order of magnitude. Separate analyses of the Xe release data are performed for each of the lattice diffusion formulas.

4.1. Release by direct lattice diffusion

Prior to embarking on data fitting using the grain-boundary diffusion model, a simpler alternative approach is tried. This approach is based on the following view of the process: even if D_{gb} were zero and the grain boundaries acted as perfect traps for fission gas, there would be some release of fission gas by direct lattice diffusion from the exposed grains at the surfaces of the specimens. For the purpose of this analysis, the following assumptions are made:

1. The surface is perfectly flat (roughness is neglected).
2. Diffusion occurs only in the UO_2 lattice in the direction (y) normal to the surface. The finite-cylinder geometry of the actual specimen is not treated.
3. The solid is infinite in the y-direction.
4. The initial concentration distribution (c_0) is uniform in y.

These restrictions lead to the familiar error-function concentration distribution:

$$c = c_0 \mathrm{erf}\left(\frac{y}{2\sqrt{Dt}}\right). \tag{11}$$

The penetration distance of the concentration disturbance is $2\sqrt{Dt}$. For the experiments reported in [36], the penetration distances using D from Eq. (9) range from 0.1 to 1.5 μm. For D from Eq. (10), the corresponding penetration distances are about a factor of three greater. All of these penetration distances are smaller than the grain diameter in the specimens, which was 8 μm. They are also less than the range of fission fragments in UO_2, which is about 7 μm.

Integrating Eq. (11) over the half-thickness L of the disk and dividing by the initial charge ($c_0 L$) yields the fractional release

$$f_{\mathrm{dir}} = \frac{4}{\sqrt{\pi}} \sqrt{\frac{Dt}{L^2}}. \tag{12}$$

The short penetration distances calculated above invalidates the fourth restriction used to obtain Eqs. (11) and (12). Direct recoil escape from depths up to the fission fragment range (μ) changes the initial condition for the diffusion problem to [40]

$$c = \begin{cases} \frac{c_0}{2}\left(1 + \frac{y}{\mu}\right), & 0 \leqslant y \leqslant \mu, \\ c_0, & y > \mu. \end{cases} \tag{13}$$

Numerical solution of the diffusion equation using Eq. (13) as the initial condition gives fractional releases that are about a factor of two smaller than those predicted from Eq. (12).

If direct lattice diffusion from surface grains is the dominant mechanism, the computed fractional releases, f_{dir}, should be the same as the measured fractional releases, f_{exp}. The first four columns of Table 1 give the experimental conditions and release fractions of the post-irradiation anneals. The next two columns give, respectively, the diffusion coefficient from Eq. (9) and the ratio $f_{\mathrm{dir}}/f_{\mathrm{exp}}$. The last two columns give the analogous information based on the diffusion coefficient of Eq. (10).

In all cases, the values of $f_{\mathrm{dir}}/f_{\mathrm{exp}}$ are less than unity by factors ranging from 4 to 100. Relaxation of restrictions 1 and 2 listed earlier could account for part of this discrepancy, but not all. This is interpreted as meaning that some other process, in particular grain boundary diffusion, enhanced the Xe release process in the experiments reported in [36].

Table 1
Comparison of experimental post-irradiation Xe release fractions [36] with simple volume diffusion theory

T (°C)	t (h)	L (cm)	f_{exp}	Low diffusivity		High diffusivity	
				D (cm^2/s)	f_{dir}/f_{exp}	D (cm^2/s)	f_{dir}/f_{exp}
1400	5	0.076	0.0016	5.4×10^{-15}	0.18	1.0×10^{-13}	0.79
1450	5	0.071	0.0020	1.1×10^{-14}	0.22	1.8×10^{-13}	0.90
1500	5	0.053	0.0081	2.0×10^{-14}	0.10	3.2×10^{-13}	0.40
1600	10	0.044	0.0180	5.8×10^{-14}	0.13	9.0×10^{-13}	0.51
1700	10	0.072	0.0400	1.5×10^{-13}	0.06	2.3×10^{-12}	0.23

4.2. Release by lattice and grain boundary diffusion with intergranular trapping

In order to rationalize the experimental fractional releases in Table 1, a model involving grain boundary diffusion coupled with grain boundary trapping and lattice diffusion is developed. The grain boundaries provide pathways for escape to the free surface of Xe released from grains in the interior of the specimen. Migration is hindered by permanent capture of Xe by intergranular traps discussed in Sections 2 and 3. Grain boundary sweeping is not considered because no grain growth was observed in the experiments utilizing stoichiometric UO_2 [36].

The grains are assumed to be spheres of radius a. During high-temperature annealing, Xe diffuses from the grain interior to the grain boundary. The grain boundaries are black sinks for Xe, which means that the Xe concentration in the solid adjacent to the grain boundary is zero. In the short-time limit, the flux of Xe to the grain boundary from inside the grain is given by [41]

$$J_g = \frac{Dc_0}{a}\left(\frac{1}{\sqrt{\pi\tau}} - 1\right), \tag{14}$$

where c_0 is the initial concentration of Xe in the grains and the dimensionless time is defined by

$$\tau = Dt/a^2. \tag{15}$$

Eq. (14) is valid for $\tau < 0.15$. This limit is applicable to most of the data analyzed. For a few points were $\tau > 0.15$, the expressions in parentheses in Eq. (14) is replaced by $2e^{-\pi^2\tau}$.

The specimen is a disk with surface-to-volume ratio S/V (which was approximated by the reciprocal of the half-thickness in Section 4.1). All surfaces, however, are assumed to face solid of infinite depth.

The polycrystalline medium is characterized geometrically by the total length of grain-boundary trace exposed in a unit area of a random section through the solid, λ, and by the total surface area of the separated grains per unit volume of solid, σ (the grain surface area in the intact solid is $\sigma/2$). For any grain shape, it can be shown that $\sigma/\lambda = 8/\pi$. For spherical grains, $\sigma = 3/a$.

Transport of Xe in the grain boundary is governed by the grain boundary diffusivity D_{gb}. In addition, the grain boundaries contain a population of traps that permanently immobilize any Xe that reaches them, either by direct lattice diffusion from the grain or by diffusion in the boundary. As in Section 2, the traps are assumed to be circular and to occupy a fraction of ϕ of the grain boundary area. The areal number density of the traps is N.

The rate of removal of mobile Xe from the grain boundary by the traps is given by the same formula that describes the sink effect of dislocations in a three-dimensional solid [42]:

$$J_{trap} = \frac{2\pi}{\ln(1/\phi)} D_{gb} c_{gb} \frac{\text{Xe atoms removed}}{s - \text{trap}}, \tag{16}$$

where c_{gb} is the local areal concentration of mobile Xe in the grain boundary. It does not include the Xe removed by the grain boundary traps. The traps are assumed to be black in the sense that the mobile Xe concentration immediately adjacent to the trap is zero.

Adding trapping to the method outlined in [13], the conservation equation for mobile Xe in the grain boundaries is given by

$$\frac{\sigma}{2}\frac{\partial c_{gb}}{\partial t} = \lambda D_{gb}\frac{\partial^2 c_{gb}}{\partial y^2} + \sigma(1-\phi)J_g - \frac{\sigma}{2}NJ_{trap}, \tag{17}$$

where the distance y is measured normal to the solid surface. In addition to Eq. (15), the following dimensionless quantities are defined:

$$X = y/a, \tag{18}$$

$$U = \frac{\pi}{8}\frac{D_{gb}}{D}\frac{c_{gb}}{ac_0}, \tag{19}$$

$$\kappa = \frac{\pi}{4}\frac{D_{gb}}{D}, \tag{20}$$

$$G = \frac{8Na^2}{\ln(1/\sqrt{\phi})}. \tag{21}$$

Neglecting ϕ compared to unity in the grain source term, Eq. (17) becomes

$$\frac{1}{\kappa}\frac{\partial U}{\partial \tau} = \frac{\partial^2 U}{\partial X^2} + \left(\frac{1}{\sqrt{\pi\tau}} - 1\right) - GU. \tag{22}$$

The initial conditions is

$$U = 0 \quad \text{at } \tau = 0, \quad \text{all } X, \tag{23}$$

which assumes that all Xe is in the grains prior to the high-temperature anneal. The boundary conditions are

$$\begin{aligned} &U = 0 \quad \text{at } X = 0, \\ &\partial U/\partial X = 0 \quad \text{at } X \to \infty. \end{aligned} \tag{24}$$

As in the direct diffusion analysis, the surface roughness is disregarded. In addition, the above formulation neglects effects such as direct release from the surface grains by lattice diffusion and the depletion of the surface region by recoil escape during irradiation. However, the action of grain boundary diffusion should allow release from greater depths than purely lattice diffusion, hence the details at the surface are less critical to the analysis than in the direct lattice diffusion calculation.

Eqs. (22)–(24) are solved for $(\partial U/\partial X)_{X=0}$ and the fractional release (f_{ind}) calculated from this solution by integrating the flux leaving the grain boundaries at the surface over time. The total quantity of Xe released from the specimen of surface area S is

$$\text{Xe released} = \lambda D_{\text{gb}} S \int_0^t \left(\frac{\partial c_{\text{gb}}}{\partial y}\right)_{y=0} \mathrm{d}t'.$$

The total Xe initially in the specimen is Vc_0, where V is the specimen volume. Dividing these two quantities and converting to dimensionless variables gives the fraction released according to the indirect route (lattice diffusion followed by grain boundary diffusion):

$$f_{\text{ind}} = 3\left(\frac{aS}{V}\right)\int_0^\tau \left(\frac{\partial U}{\partial X}\right)_{X=0} \mathrm{d}\tau'. \tag{25}$$

The following analytical solution for the surface gradient is developed in Appendix A:

$$\left(\frac{\partial U}{\partial X}\right)_{X=0} = \sqrt{\kappa}\exp\left(-\frac{1}{2}G\kappa\tau\right) I_0\left(\frac{1}{2}G\kappa\tau\right) - \frac{\operatorname{erf}\left(\sqrt{G\kappa\tau}\right)}{\sqrt{G}}, \tag{26}$$

where I_0 is the modified Bessel function of the first kind of order zero. This solution is restricted to $\tau < 0.15$ because of the short-time approximation for the Xe flux to the grain boundary from the grains as expressed by Eq. (14). For larger values, Eqs. (22)–(24) are solved numerically.

In the absence of trapping ($G = 0$), Eq. (26) is sufficiently simplified that the integral in Eq. (25) can be performed analytically. The resulting theoretical fractional release is

$$f_{\text{ind}}^{(G=0)} = 3\left(\frac{aS}{V}\right)\sqrt{\kappa}\left(\tau - \frac{4}{3\sqrt{\pi}}\tau^{3/2}\right). \tag{27}$$

The interesting feature of this result is the absence of the $\sqrt{\tau}$ time dependence usually associated with diffusional processes (e.g. Eq. (12) for the direct release mechanism).

The above indirect release model was fitted to the data given in the first four columns of Table 1. Separate data fitting was performed for the 'low' and 'high' lattice diffusivities of Eqs. (9) and (10). Two of the fitting parameters are the pre-exponential factor and the activation energy of the κ parameter defined by Eq. (20) and expressed as

$$\kappa = \kappa_0 \mathrm{e}^{T_\kappa/T}. \tag{28}$$

The form of this equation assumes that the activation energy of D_{gb} is lower than that of D [1]. The quantity T_κ is the activation energy of the ratio D_{gb}/D divided by the universal gas constant.

The third fitting parameter is the quantity G defined by Eq. (21). This parameter was assumed to be the same at all temperatures and to remain constant during the time at temperature. That is, the microstructure of the intergranular traps was not permitted to anneal during the release process.

Experience in the fitting process showed that instead of κ_0, error minimization was much more sensitive to the value of κ at a temperature in the middle of the experimental range (1500°C). Thus, the actual fitting parameters were G, T_κ, and

$$\log \kappa(1773) = \log \kappa_0 + \frac{T_\kappa}{2.3 \cdot 1773}. \tag{29}$$

Fitting of the data proceeded in the following fashion:

- Select a lattice diffusivity (low or high).
- Fix the parameter G, starting at $G = 0$.
- Vary $\log \kappa(1773)$ and T_κ until the error measure or objective function defined in Eq. (30) is a minimum.
- Increase the parameter G and repeat error minimization.

$$\text{error} = \frac{1}{5}\sum_1^5 \left|\frac{f_{\text{ind}} - f_{\text{exp}}}{f_{\text{exp}}}\right|. \tag{30}$$

The above process is terminated when the minimum error starts to increase above the low-G limiting value.

Table 2 shows the results of fitting the data to the indirect release model with the low lattice diffusion coefficient.

Equally satisfactory agreement of the model and the data (i.e. the same minimum error) was achieved for all

Table 2
Results of fitting Xe release data to the indirect model using the low lattice diffusivity formula

G	Minimum error	$\log \kappa(1773)$	T_κ (K)
0	0.23	3.80 ± 0.01	28000 ± 500
0.01	0.24	3.84 ± 0.02	23000 ± 1300
0.02	0.24	3.92 ± 0.01	22000 ± 700
0.1	0.36	4.14 ± 0.04	5000–30000

values of the grain boundary trap parameter $G \leqslant 0.1$. The minimum error increases rapidly for larger G values.

Similar results have been obtained by means of the general Levenberg–Marquard method (implemented in the software PEST [44]), or when applying the absolute difference between theory and data as the objective function. Both approaches gave results with a better fit to the large release fraction experiments than obtained with the error based on the fractional difference as in Eq. (30), in contrast with the fit for the low temperature data points. Nevertheless, the results indicated that the experimental data do not support a two-step diffusional model that is accompanied by strong intergranular trapping of Xe. By way of comparison, Eq. (21) shows that the point in Figs. 1 and 2 for the least efficient trap microstructure (i.e. $N = 0.1\ \mu m^{-2}, \phi = 0.01$) has a trapping parameter $G = 5.6$. The data from [36] are consistent with gas release by sequential lattice and grain boundary diffusion unimpeded by trapping at natural intergranular defects.

The last two columns in Table 2 give the grain boundary diffusivity parameters associated with the best fit of the data. As suggested by the small error bars, the minimum error is well defined in the coordinate represented by $\log \kappa(1773)$; the average value of this parameter in the range $0 < G < 0.1$ is 3.85 ± 0.01. This gives a reasonable reliable value of $D_{gb} = 1.6 \times 10^{-10}$ cm^2/s at 1773 K.

The activation energy of κ is contained in the last column of Table 2. The uncertainty in T_κ is even greater than implied by the error bars associated with this parameter at a fixed G. The error measure of Eq. (30) can be thought of as a surface dependent on the two κ fitting parameters. The minimum error on such a surface lies along a trough with the walls rising sharply in the $\log \kappa(1773)$ direction but running like a canyon floor in the T_κ direction. For example, error measures just 0.02 greater than the minimum values shown in the table are obtained over a range $1000 < T_\kappa < 30000$. With this caveat, accepting the average value of 24000 K from the first three rows of Table 2 yields a grain boundary diffusivity of

$$D_{gb}^{(\text{low } D)} = 9 \times 10^{-8} \exp(-92/RT)\ \text{cm}^2/\text{s}, \quad \text{AE in kJ/mol.} \tag{31}$$

Table 3
Results of fitting Xe release data to the indirect model using the high lattice diffusivity formula

G	Minimum error	$\log \kappa(1773)$	T_κ (K)
0	0.26	1.42 ± 0.03	2440 ± 580
0.01	0.27	1.45 ± 0.04	1350 ± 340
0.02	0.27	1.43 ± 0.03	1620 ± 470
0.1	0.28	1.44 ± 0.03	1770 ± 430
0.2	0.28	1.58 ± 0.05	1620 ± 450
0.5	0.35	1.74 ± 0.04	1730 ± 450
1.5	0.43	2.02 ± 0.13	800–15000
5.0	0.62	2.36 ± 0.07	800–15000

The accuracy of this equation is high at $T = 1773$ K but Eq.(31) is much less reliable at other temperatures.

If the high lattice diffusivity (Eq. (10) is used in fitting the data to the indirect release model, Table 3 shows that a constant minimum error is achieved for all $G \leqslant 0.5$. In this range of G, the error measure is quite sensitive to the $\log \kappa(1773)$ parameter but quite insensitive to the activation energy parameter T_κ. The grain boundary diffusivity deduced from the value of $\log \kappa(1773) = 1.43$ at the minimum error is $D_{gb} = 1.1 \times 10^{-11}$ cm^2/s at 1773 K, which is a factor of 15 smaller than the corresponding value obtained using the low lattice diffusivity in the data analysis.

Taking the average of the entries in the last column of Table 3 ($T_\kappa \sim 1800$ K), the temperature dependence of the Xe grain boundary diffusivity is obtained as

$$D_{gb}^{(\text{high } D)} = 1.3 \times 10^{-3} \exp(-272/RT)\ \text{cm}^2/\text{s}. \tag{32}$$

As in the low lattice diffusivity analysis, the temperature dependence implied by this result is much less reliable than the value of D_{gb} at 1773 K.

The significant difference between the D_{gb} formulas deduced from the data is entirely due to the order-of-magnitude discrepancy in D from Eqs. (9) and (10).

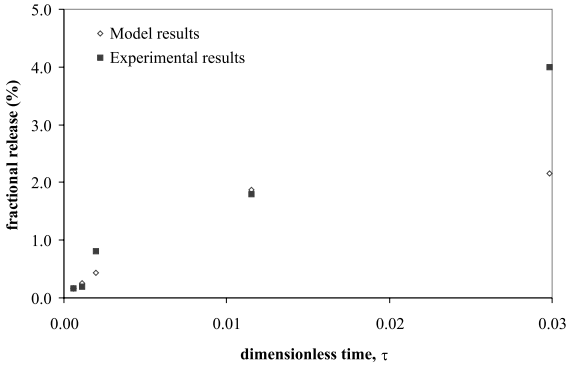

Fig. 3. Comparison of model results ($G = 0$, $\log \kappa(1773) = 3.80$, $T_\kappa = 27500$ K) with experimental data using Eq. (9) for D.

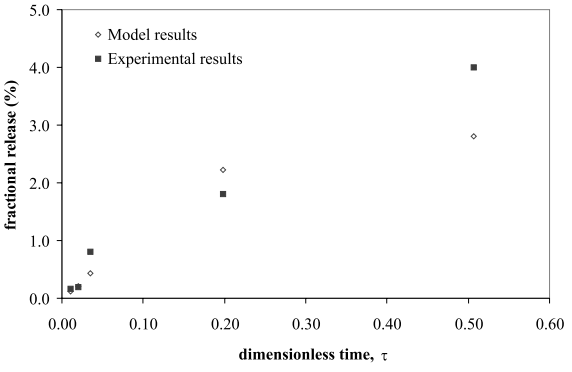

Fig. 4. Comparison of model results ($G = 0$, $\log \kappa(1773) = 1.41$, $T_\kappa = 1030$ K) with experimental data using Eq. (10) for D.

Figs. 3 and 4 compare the Xe release data with the minimum-error indirect model predictions for the two lattice diffusivities employed in the fitting process. The theoretical points neglect intergranular trapping, although essentially the same results are obtained for any G less than the values in Tables 2 and 3 where the minimum error begins to rise. The quality of the agreement between theory and experiment (as gauged by Eq. (30)) is roughly the same for the low and high lattice diffusion coefficient formulas. For either D, the indirect model cannot reproduce the experiment release fractions at the longest dimensionless time τ. The predicted increase in f_{ind} between the last two τ values is small because the difference in the thickness of the specimens counteracts the effect of temperature on the diffusion coefficient. We suspect that the last experimental points give too large a fractional release.

5. Conclusions

The objective of this paper is to provide answers to the two questions concerning release of fission gas from polycrystalline UO_2 that were posed at the end of Section 1.

The first question concerned the mean migration distance of a Xe atom in a grain boundary decorated with a population of perfect-absorbing circular traps characterized by the areal number density and fractional coverage. For values of these two parameters that roughly encompass the intergranular gas bubble populations observed in irradiated fuel, a Xe atom will be trapped after a migration distance in the grain boundary equal to the size of a grain (~ 8 μm) or less. This result simply provides a theoretical justification for the universal rejection of grain boundary transport as a release mechanism for fission gases in irradiated UO_2 fuel.

The second question deals with the numerous laboratory experiments of the 'post irradiation anneal' type utilizing trace-irradiated UO_2. These specimens do not exhibit intergranular porosity because the gas concentration is too low to nucleate bubbles. However, natural microstructural defects or impurities in the grain boundaries of fresh UO_2 may play the same trapping role as do bubbles in irradiated fuel. To investigate this possibility, recent data on Xe release from stoichiometric trace-irradiated UO_2 disks were analyzed by two models. The first approach, called the direct release model, neglects intergranular transport and ascribes gas release solely to lattice diffusion from solid at the surface of the specimens. The predicted release fractions were far smaller than the observations, suggesting the need for a mechanism that allows transport from deeper within the specimens.

The second, indirect model posits release from the grains by lattice diffusion followed by transport to the free surface by intergranular diffusion. This model had previously been successfully applied to Te and I release, but its applicability to the rare gases has been generally rejected (at least for power-reactor fuel). The indirect release model was modified to account for intergranular trapping of Xe, since this process was believed to be the principal reason why the rare gases are retained in irradiated fuel for substantial burnups.

Comparison of the indirect model with the Xe release data involved adjustment of three parameters: two for D_{gb} and a third parameter representing the intergranular traps. The best agreement between theory and experiment was achieved for little or no trapping, or at least for G values an order of magnitude smaller than those representing bubble populations observed by fractography of irradiated fuel. The fitting procedure fairly accurately fixed D_{gb} at 1500°C, but was unable to determine a reliable activation energy for this property.

The grain boundary diffusion coefficients deduced from application of the indirect model to this small set of data are no more accurate than the lattice diffusivities of Xe in UO_2 needed in the calculation. The uncertainty in this property is at least one order of magnitude; it affects not only the specific application treated in this paper but all mechanistic fission gas behavior codes, a point which the authors of theses codes do not address.

Acknowledgements

One of the authors (P.V.U.) is very grateful to Dr J.A. Turnbull (UK), Professor V. Sobolev (Moscow Engineering Physics Institute), Dr M. Lippens (S.A.BELGONUCLEAIRE) and Dr M. Verwerft (SCK·CEN) for their valuable discussions and interest in this work. The useful comments provided by Professor Hj. Matzke (Institute for Transuranium Elements) and Professor P. Chambré (University of California) are also acknowledged.

Appendix A

Eq. (22) is first transformed using the new variables:

$$\theta = \kappa\tau, \tag{A.1}$$

$$V = \frac{e^{G\theta}}{\sqrt{\kappa}} U, \tag{A.2}$$

which leads to

$$\frac{\partial V}{\partial \theta} = \frac{\partial^2 V}{\partial X^2} + \frac{e^{G\theta}}{\sqrt{\pi\theta}} - \frac{e^{G\theta}}{\sqrt{\kappa}}. \tag{A.3}$$

Eq. (A.3) is solved by the Laplace transform method with the same initial and boundary conditions as U (Eqs. (23) and (24)). The subsidiary equation for (A.3) is

$$\frac{d^2\tilde{V}}{dX^2} - p\tilde{V} = -\frac{1}{\sqrt{p-G}} + \frac{1}{\sqrt{\kappa}}\frac{1}{p-G}. \tag{A.4}$$

Solving for the transform of V and taking the gradient at $X = 0$ gives

$$\left(\frac{d\tilde{V}}{dX}\right)_{X=0} = \frac{1}{\sqrt{p}\sqrt{p-G}} - \frac{1}{\sqrt{\kappa}}\frac{1}{\sqrt{p}(p-G)}. \tag{A.5}$$

The Bateman tables [43] provide the inverse transform of the second term on the right-hand side of (A.5). For the first term on the right, invoking the convolution property of the Laplace transform yields

$$L^{-1}\left[\frac{1}{\sqrt{p}\sqrt{p-G}}\right] = \frac{1}{\pi}\int_0^\theta \frac{e^{Gs}}{\sqrt{s}\sqrt{\theta-s}}\,ds = \exp\left(\frac{1}{2}G\theta\right) I_0\left(\frac{1}{2}G\theta\right), \tag{A.6}$$

where I_0 is the modified Bessel function of the first kind of zero order. Assembling these results gives

$$\left(\frac{\partial U}{\partial X}\right)_{X=0} = \sqrt{\kappa}e^{-G\theta}\left(\frac{\partial V}{\partial X}\right)_{X=0} = \sqrt{\kappa}\exp\left(-\frac{1}{2}G\theta\right) I_0\left(\frac{1}{2}G\theta\right) - \frac{\operatorname{erf}(\sqrt{G\theta})}{\sqrt{G}}. \tag{A.7}$$

References

[1] T. Kaur, Y. Mishin, W. Gust, Fundamentals of Grain and Interphase Boundary Diffusion, 3rd Ed., Wiley, New York, 1995.
[2] P. Shewmon, Diffusion in Solids, 2nd Ed., Minerals, Metals and Materials Society, 1980.
[3] K. Une, S. Kashibe, J. Nucl. Mater. 232 (1996) 240.
[4] A.J. Flipot, H. Van Den Broeck, A. Delbrassine, R. Gilissen, Nucl. Eng. Int. 15 (1971) 345.
[5] G.R. Chilton, J. Edwards, J. Nucl. Mater. 78 (1978) 182.
[6] J.A. Turnbull, C.A. Friskney, J. Nucl. Mater. 58 (1975) 31.
[7] M.V. Speight, J.A. Turnbull, J. Nucl. Mater. 68 (1977) 244.
[8] J.A. Turnbull, C.A. Friskney, F.A. Johnson, A.J. Walter, J.R. Findlay, J. Nucl. Mater. 67 (1977) 301.
[9] R. Carroll, O. Sisman, Nucl. Appl. 2 (1966) 142.
[10] A.H. Booth, AECL Report CRDC-721, 1957.
[11] M. Gardani, C. Ronchi, Nucl. Sci. Eng. 107 (1991) 315.
[12] D.R. Olander, V. Nubayi, J. Nucl. Mater. 270 (1999) 1.
[13] D.R. O1ander, Adv. Ceram. 17 (1986) 271.
[14] U.M. EI-Saied, D.R. Olander, J. Nucl. Mater. 207 (1993) 313.
[15] Y. Guérin, J. Noirot, D. Lespiaux, C. Struzik, P. Garcia, P. Blanpain, G. Chaigne, Microstructure evolution and in-reactor behaviour of MOX fuel, in: Proceedings of the International Topical Meeting on Light-Water Reactor Fuel Performance, American Nuclear Society, Park City, UT, 2000, p. 1023.
[16] R.J. White, M.O. Tucker, J. Nucl. Mater. 118 (1983) 1.
[17] R.J. White, A new mechanistic model for the calculation of fission gas release, in: Proceedings of the International Topical Meeting on Light-Water Reactor Fuel Performance, American Nuclear Society, West Palm Beach, FL, 1994, p. 196.
[18] Y.H. Koo, D.S. Sohn, Y.K. Yoon, J. Nucl. Mater. 209 (1994) 62.
[19] OECD, NEA Nuclear Science Committee Task Force, Scientific issues in fuel behaviour, 1995.
[20] A. Denis, R. Piotrkowski, J. Nucl. Mater. 229 (1996) 149.
[21] L.C. Bernard, E. Bonnaud, J. Nucl. Mater. 244 (1997) 75.
[22] P. Lösönen, Modeling steady state fission gas release at high burnup, in: Proceedings of the International Topical Meeting on Light-Water Reactor Fuel Performance, American Nuclear Society, Park City, UT, 2000, p. 289.
[23] C.T. Walker, P. Knappik, M. Møgensen, J. Nucl. Mater. 160 (1988) 10.
[24] C.T. Walker, M. Møgensen, J. Nucl. Mater. 149 (1987) 121.
[25] M.O. Tucker, Rad. Eff. 53 (1980) 251.
[26] K. Une, S. Kashibe, J. Nucl. Sci. Technol. 27 (1990) 1002.
[27] M. Møgensen, C. Bagger, C.T. Walker, J. Nucl. Mater. 199 (1993) 85.
[28] T. Kogai, J. Nucl. Mater. 244 (1997) 131.
[29] W.R. Grimes, C.R.A. Catlow, Philos. Trans. Roy. Soc. London A 335 (1991) 609.
[30] P. Van Uffelen, Contribution to the modelling of fission gas release in light water reactor fuel, PhD thesis, Nuclear Engineering Department, University of Liège, Belgium, 2000.
[31] P. Van Uffelen, J. Nucl. Mater. 280 (2000) 275.
[32] F.S. Ham, J. Appl. Phys. 30 (6) (1959) 915.
[33] S. Kashibe, K. Une, J. Nucl. Sci. Technol. 28 (1991) 1090.
[34] I. Zacharie, S. Lansiart, P. Combette, M. Trotabas, M. Coster, M. Groos, J. Nucl. Mater. 255 (1998) 92.
[35] S.G. Prussin, D.R. Olander, W.K. Lau, L. Hansson, J. Nucl. Mater. 154 (1988) 25.
[36] M.A. Mansouri, D.R. Olander, J. Nucl. Mater. 254 (1998) 22.

[37] Hj. Matzke, J. Chem. Soc., Farad. Trans. 86 (1990) 1.
[38] D. Davies, G. Long, AERE Report 4347, 1963.
[39] R.M. Cornell, Philos. Mag. 19 (1969) 539.
[40] B.J. Lewis, J. Nucl. Mater. 148 (1978) 28.
[41] D.R. Olander, Fundamental Aspects of Nuclear Reactor Fuel Elements, Section 15.5.1, National Techn. Info Services, 1976.
[42] D.R. Olander, Fundamental Aspects of Nuclear Reactor Fuel Elements, Section 13.5.2, National Techn. Info Services, 1976.
[43] H. Bateman, Tables of Integral Transforms, vol. 2, McGraw-Hill, New York, 1954.
[44] J. Doherty, PEST: Model-Independent Parameter Estimation, Watermark Computing, 1998.